De-signature of a dual string marine seismic source

Rob Telling, Stuart Denny, Sergio Grion & R. Gareth Williams, Shearwater GeoServices*

Summary

We estimate far-field signatures for a dual-string array in a triple-source configuration and evaluate shot-by-shot directional de-signature performance on a test line of seismic data acquired in the Barents Sea. In particular we examine resilience of our methods to a severe gun drop-out scenario. Optimized signatures are derived by least-squares inversion with near-field hydrophone measurements as input. This approach has proven to be a robust approach for broadband surveys carried out with conventional three-string dual-source arrays. The use of smaller sources with fewer elements enables more flexible acquisition but there is a potential for greater sensitivity to drop-out of any given element and, with fewer associated near-field hydrophone measurements, increased sensitivity of the inversion to noise. Despite these concerns, we obtain good quality signatures with comparable de-signature performance for both the reference case and the array suffering from a simulated gun drop-out condition.

Introduction

Marine source signature estimation using near-field hydrophone measurements is a well-established procedure and is now recognized as important for accurate broadband de-signature of seismic data. An example of modern far-field signature estimation is the least-squares technique of Hargreaves et al. (2015, 2016), which uses near-field hydrophone (NFH) data as inputs and builds on the original work of Ziolkowski *et al.* (1982) and Parkes *et al.* (1984).

Signature estimation and de-convolution for tuned and de-tuned air-gun arrays are also the subject of an investigation by Ziolkowski (1987) but at that time the de-convolution was limited to the band 10-100 Hz. In this work we extend the analysis to broadband seismic data with a good signal-to-noise ratio in the range ~2-200 Hz; we also assess de-bubble performance at low frequency, as well as accurate representation of the source ghost at the high-frequency end. We refer to Telling *et al.* (2018) for details on the signature estimation and rationale for optimizing reflectivity and focus here on a gun drop-out scenario including de-signature results for pre-stack and stacked data when the changes in the source signature are handled correctly and when they are not.

The results we present on far-field signature estimation and de-signature processing are for an array that is smaller than typically used, having 12 elements on two strings instead of the perhaps more typical 18 elements on three strings. It is therefore potentially more sensitive to gun drop-out and to proportionately fewer near-field measurements as input. These have the potential to impact signature estimation quality since the noise is at a more-or-less similar level. Waves in the ocean environment cause acoustic noise on the NFH measurements, and create uncertainty in the coordinates and depths of source elements in the array.

Methodology

A single 15 km test line was shot with a reference array and a de-tuned array firing alternately. The resulting common-mid-point (CMP) lines are nominally 25m apart. The reference source array had 12 source elements containing 18 active guns on two strings, totaling 2965 cubic inches. The de-tuned variant, representing a source drop-out condition worse than normally allowed in quality control specifications, had 16 active guns, totaling 2415 cubic inches. Compared to the reference array, traditional source modelling of this drop-out condition showed an amplitude drop of 7.8%, a primary-bubble ratio drop of 53%, a normalized correlation coefficient of 0.976, an average spectral deviation of 1.2 dB in the 10 – 70 Hz band, and a maximum spectral deviation of 7.4 dB in the 10 – 70 Hz band. Both sources were deployed at 7 m and operated at 2000 PSI. Seismic data were acquired via a twelve streamer spread. During the test data acquisition in the Barents Sea the crew noted a significant wave height of 1 m.

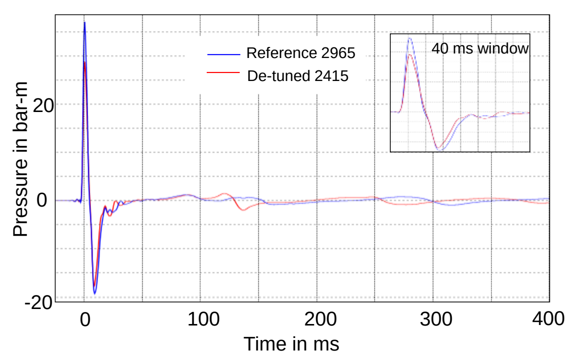

Figure 1 – Optimized vertical far-field signatures for the reference 2965 cubic inch array (blue) and de-tuned 2415 cubic inch array (red). Note the lower peak pressure for the de-tuned array, and more prominent bubble pulse.

We estimated signatures for both the reference array and the de-tuned array after optimization of ghosting parameters (Hargreaves *et al.* 2016, Telling *et al.* 2018). These were compared with the seabed extracted wavelet as a check. We then derived directional de-signature operators and applied them to seismic records using a τ-p based de-convolution which encapsulates source de-ghosting and de-bubble via an operator that matches the supplied directional source signatures to a zero-phase Ormsby wavelet. This was applied to the data shot with the reference source and also that shot with the de-tuned source. In the case of the de-tuned source we look at two separate cases to highlight the value of accurate shot-by-shot de-signature: 1) we assume the nominal tuned source signature is still valid – in essence the worst-case error when the drop-out is not handled correctly and 2) we use the correct NFH data to handle the drop-out.

Results

Optimized directional signatures were estimated at take-off angles from -30 to +70 degrees and are shown for the case of vertical incidence in Figure 1. The corresponding spectra are shown in Figure 2.

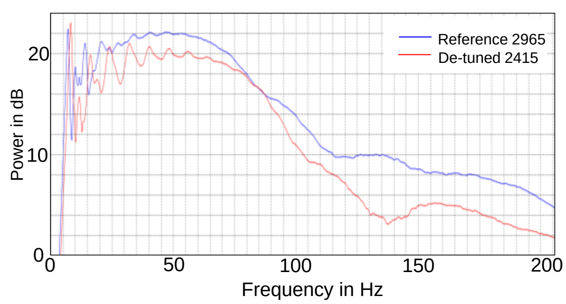

Figure 2 – Spectra for the estimated far-fields at vertical incidence shown in Figure 1. Note the lack of a prominent ghost notch – expected in the vicinity of 107 Hz for 7 m array – indicating a weaker source ghost than expected for the given sea-state.

As a comparison, the source wavelet was also estimated by flattening the sea-bed reflection on the near trace data and extracting a mean signature. Comparisons of the NFH-derived signatures with the (receiver-side) de-ghosted extracted wavelet are shown in Figure 3 and Figure 4 for the 2965 reference array and 2415 de-tuned array respectively (which correspond to adjacent common mid-point lines). The results show good general agreement in terms of ghost timing and relative amplitude.

The pre-stack data before and after de-signature are shown in Figure 5 and stacked data in Figure 6 together with associated spectra in Figure 7. These data include the pathological case that serves to illustrate the effect of not reacting to a drop-out i.e. using a nominal signature for the array derived at the start of the survey.

The pre-stack and stacked results support the case that when shot-by-shot NFH-derived signatures are used the results after de-signature are of good quality and crucially, that the two datasets obtained using different sources are comparable – see 2nd and 4th panels in Figure 5 and the invisible join in the bottom image in Figure 6. They are not identical, as evidenced in the spectra in Figure 7. This is partly related to the fact that we are dealing with CMP lines separated by 25 m, leading to differences in cross-line ghosting take-off and arrival angles, but it may also be due to features that are not fully captured in either of the estimated far-fields, leaving residual differences after de-signature.

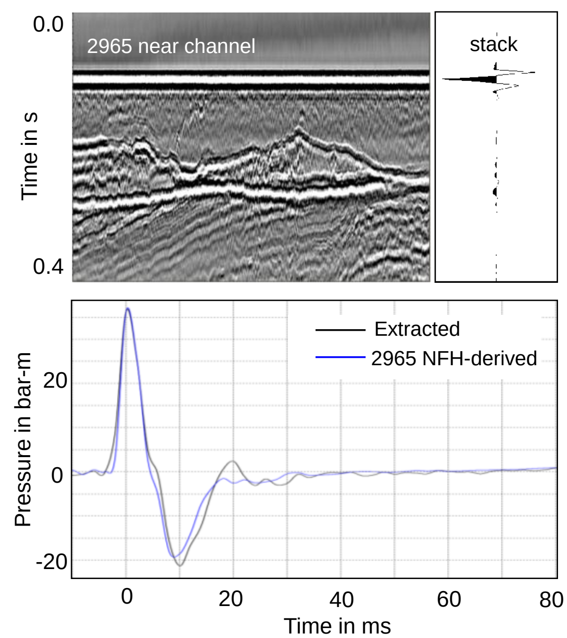

Figure 3- Near-trace data flattened on sea-bed (top left) used to extract mean wavelet (top right), then compared after receiver-side de-ghosting (black curve, bottom) with the NFH-derived signature for the 2965 de-tuned array (blue curve).

Conclusions

Optimized far-field signatures were estimated for two different dual-string source arrays using NFH data. One of these arrays was de-tuned to represent a severe gun-drop-out condition. In both cases the signatures compared well with sea-bed extracted wavelets, carried-out as an independent check on the parameterization of the ghosting at the sea-surface. We then derived directional de-signature operators on a shot-by-shot basis and applied these over a 15 km sequence of seismic data.

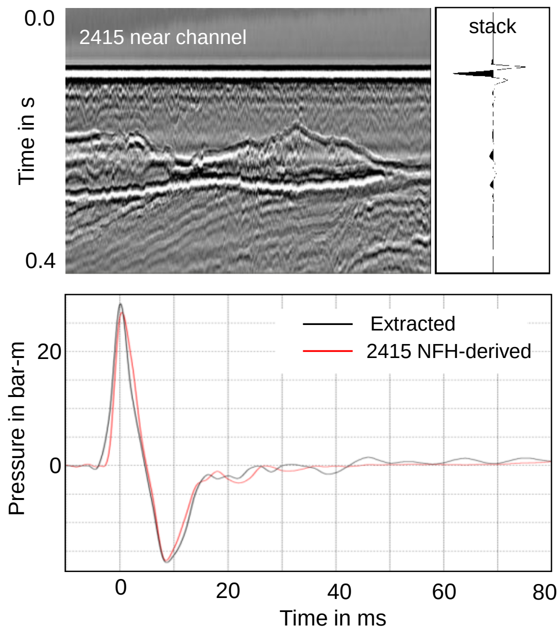

Figure 4 – Near-trace data flattened on sea-bed (top left) used to extract mean wavelet (top right), then compared after receiver-side de-ghosting (black curve, bottom) with the NFH-derived signature for the 2415 de-tuned array (red curve).

After de-signature processing, comprising de-ghosting, de-bubble and zero-phasing, the data appears of good quality with no obvious artifacts and the two datasets shot with different sources become comparable.

To illustrate the importance of a capability to deal with changes in signature on a shot-by-shot basis, we demonstrated the type of artifacts produced when using a nominal source signature for the array with two guns dropped-out. Overall, our results support the conclusion that it is possible to obtain good signatures for dual string arrays, despite fewer hydrophone measurements in the near field and increased susceptibility to the loss of source elements, provided the signatures are calculated shot-by-shot. There may still be scope to improve signature estimation accuracy and resulting de-signature. We believe increasing the number of measurements in the near-field would help in this regard and also has the advantage of allowing better treatment of the source ghost (Parkes and Hatton, 1986, Telling *et al.* 2018).

Acknowledgements

We thank the crew of the *Polar Empress* for their work in carrying out this test and are grateful to Wintershall Norge AS and partners for permission to show these data.

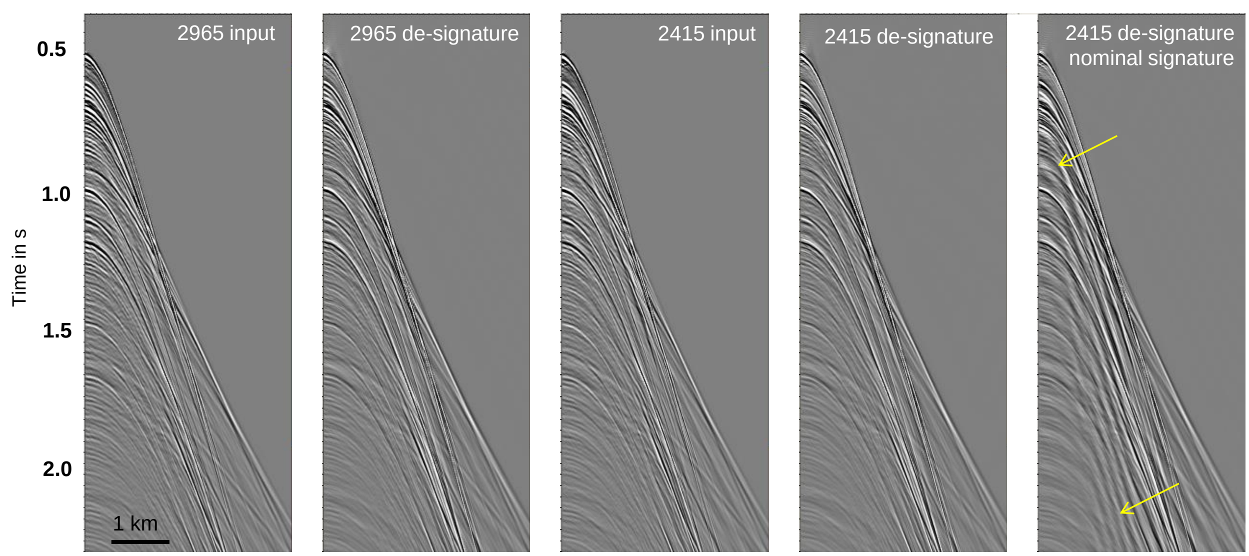

Figure 5 – Pre-stack data before and after de-signature showing the input data shot by each array and the resulting de-signature using NFH-derived signatures on a shot-by-shot basis. The rightmost panel shows what happens if the nominal array signature (2965) is used on the data shot with the 2415 array i.e. a simulated drop-out scenario which is not handled correctly. Yellow arrows highlight residual bubble energy.

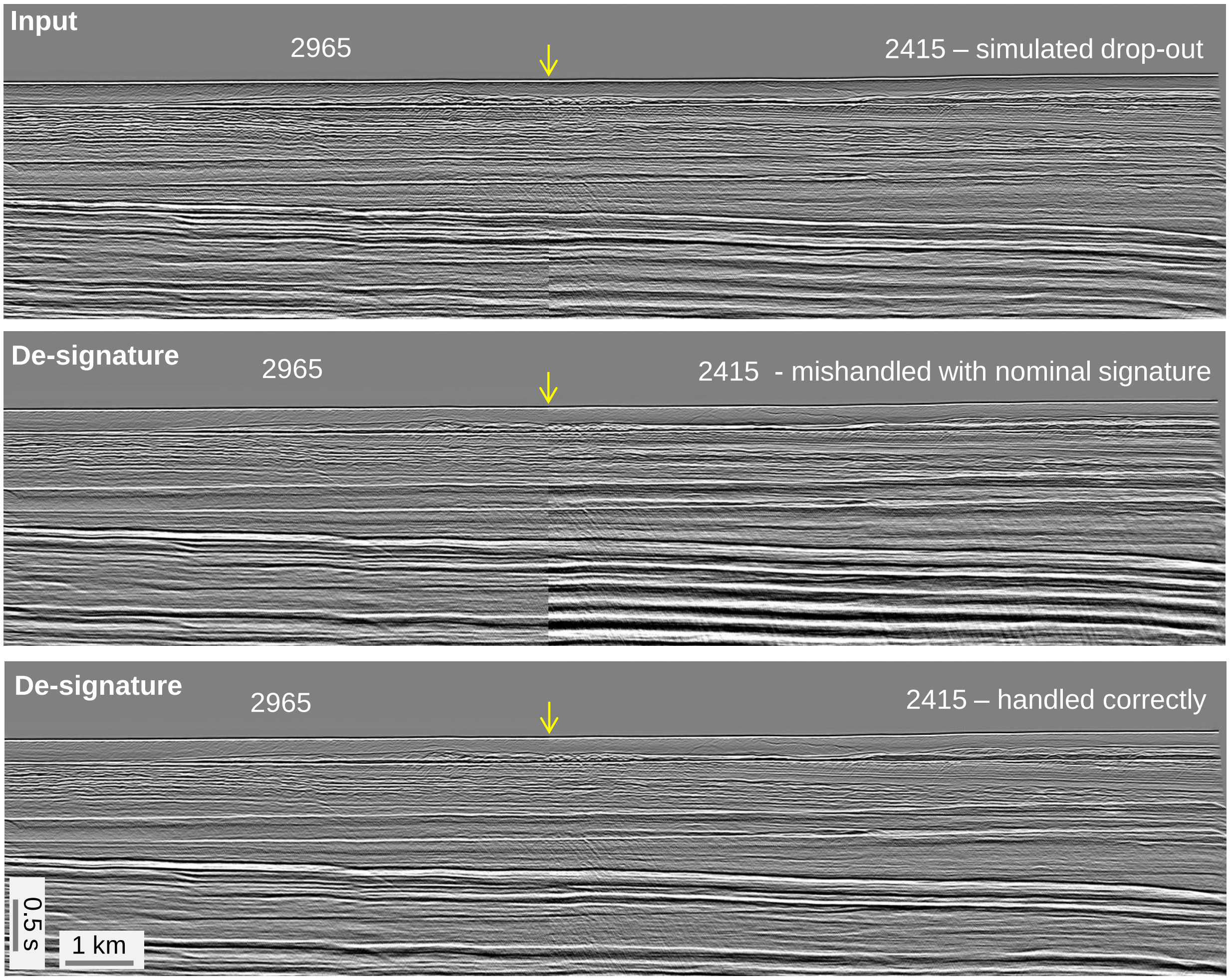

Figure 6 – A composite of stacked data before (top) and after de-signature (middle and bottom) illustrating the benefit of adapting to changes in the array and associated signature on a shot-by-shot basis rather than using a nominal signature. The yellow arrow indicates the join of the datasets shot using the 2965 reference array and the dataset shot with the 2415 array.

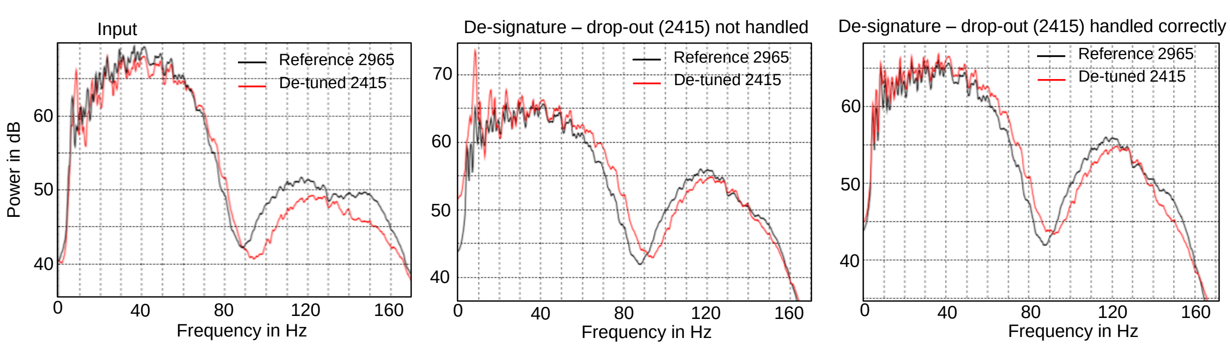

Figure 7 – Logarithmic power spectra corresponding to the stacked data in Figure 6. The red curve in the central image highlights the mis-handling of the de-signature, particularly the bubble energy peak around 8 Hz.

References

Hargreaves, N., Grion, S. and Telling, R. [2015]. Estimation of air-gun array signatures from near-gun measurements - least-squares inversion, bubble motion and error analysis. *85th SEG Meeting* Expanded Abstracts, 149-153.

Hargreaves, N., Telling, R., Grion, S. [2016]. Source deghosting and directional designature using near-field derived airgun signatures. *78th EAGE Conference and Exhibition*, Extended Abstracts

Parkes, G. E., Ziolkowski, A., Hatton, L. and Haugland, T. [1984]. The signature of an airgun array: computation from near-field measurements including interactions — Practical considerations. *Geophysics*, **49**, 105–111

Parkes, G. and Hatton, L. [1986] The Marine Seismic Souce. D. Reidel, Dordrecht

Telling, R. H., Light, R., Grion, S., Denny, S. and Williams, R. G. [2018] Signature estimation and drop-out implications for a triple source marine seismic survey *80th EAGE Conference and Exhibition*, Extended Abstracts

Ziolkowski, A., Parkes, G., Hatton, L. and Haugland T. [1982]. The signature of an air gun array: Computation from near-field measurements including interactions. *Geophysics*, **47** (10), 1413-1421.

Ziolkowski, A. [1987].The determination of the far-field signature of an interacting array of marine seismic sources from near-field measurement – results from the Delft air gun experiment. First Break, 5 (1), 15-29